Bioorganic Chemistry 88 (2019) 102930

Contents lists available at ScienceDirect

Bioorganic Chemistry

journal homepage: www.elsevier.com/locate/bioorg

Synthesis and biological evaluation of 3-functionalized 2-phenyl- and 2-alkylbenzo[*b*]furans as antiproliferative agents against human melanoma cell line

Halina Kwiecień[a,*], Magdalena Perużyńska[b], Karolina Stachowicz[a], Katarzyna Piotrowska[c], Joanna Bujak[c], Patrycja Kopytko[c], Marek Droździk[b]

[a] West Pomeranian University of Technology in Szczecin, Department of Organic Synthesis and Drug Technology, Al. Piastów 42, 71-065 Szczecin, Poland
[b] Pomeranian Medical University, Department of Experimental & Clinical Pharmacology, Powstańców Wlkp. 72, 70-111 Szczecin, Poland
[c] Pomeranian Medical University, Department of Physiology, Powstańców Wlkp. 72, 70-111 Szczecin, Poland

ARTICLE INFO

Keywords:
Benzo[*b*]furans
Acylation
Anti-tubulin agents
Antitumor agents
Melanoma A375 cell line

ABSTRACT

The key function of microtubules and mitotic spindle in cell division make them attractive targets in anticancer therapy. In the present study, functionalized in 3 position 2-phenyl- and 2-alkylbenzo[*b*]furans were synthesized and evaluated as antitumor agents. Among the synthesized derivatives **13a**, **13b and 14** exhibited the most potent antiproliferative activity against human melanoma A375 cell line with IC_{50} values of 2.85 μM, 0.86 μM, 0.09 μM, respectively. The most promising compound defined was **14** with three methoxy groups in the 3-aroyl substituent and 7-methoxy group in 2-phenylbenzo[*b*]furan skeleton. Tubulin polymerization assay, confocal microscopy imaging and flow cytometry analysis revealed that 2-phenyl-3-aroylbenzo[*b*]furans (**13a, 13b and 14**) inhibited tubulin polymerization leading to disruption of mitotic spindle formation, cell cycle arrest in G2/M phase and apoptosis.

1. Introduction

The majority of naturally derived anticancer drugs inhibit cell proliferation by acting on spindle microtubules. Microtubules are protein biopolymers formed through polymerization of heterodimer subunit of α- and β-tubulin. The polymerization is reversible, and the microtubule/tubule dynamics are involved in a number of cell functions, including cell division, migration, and shape change. Rapid microtubule dynamics are especially prominent in mitosis, and are essential for proper spindle assembly and function [1]. Disruption of microtubule dynamics leads to cell apoptosis. A number of known antimitotic agents act by binding to the protein tubulin, an α, β-heterodimer that forms the core of the microtubule. Vinica alkaloids, including vinblastine and vincristine as well as colchicine inhibit microtubule polymerization. In contrast, taxanes, including paclitaxel, as well as laulimaide bind to polymerized microtubules at the inner surface of the β subunit and promote tubulin stabilization [2,3]. The recent literature reports show that tubulin dynamics is still a promising target for new anticancer agents [4–8]. Most of antimitotic agents interact with tubulin through at least four major binding sites: the laulimalide, vinica alkaloid, taxane, and colchicine site [2,9,10]. In contrast to targeting the taxane or vinca alkaloid binding sites, more attention has been drawn to develop inhibitors of colchicine site, due to its potential antimitotic and vascular disrupting properties. Such vascular disrupting agents take advantage of the significant differences that exist between the normal, healthy tissues and tumour vasculature [11].

Colchicine (**1**, Fig. 1) inhibits microtubule assembly (antimitotic properties have been known for over 50 years), but the therapeutic value of colchicine activity against cancer is restrained by its toxicity and low therapeutic index. The significant toxicity of colchicine is attributed to its very slow dissociation from tubulin, which leads to its persistence in sensitive tissues for several days [12]. Although colchicine is not used as anticancer agent, there have been multiple efforts to clinically develop colchicine binding site agents. Most known agents that bind to the colchicine site often have shorter half-lives *in vivo* and are much better tolerated. Combretastatin (**2**, Fig. 1) and phenstatin (**3**) (combretastatin-analog with the double bond of being replaced by a carbonyl group) are examples of reversible binders to the colchicine site that have short half-lives *in vivo* and that are much better tolerated than colchicine [13–15]. BNC-105 (**5**), phenstatin analogue with the benzene ring of phenstatin replaced by benzofuran, exhibits selectivity for growth factor activated endothelial cells [16]. Phenstatin (**3**) and BNC-105 (**5**) have entered clinical trials, where they were administered as the soluble disodium phosphate ester prodrugs **4** and **6** which were

* Corresponding author.
E-mail address: halina.kwiecien@zut.edu.pl (H. Kwiecień).

https://doi.org/10.1016/j.bioorg.2019.102930
Received 27 August 2018; Received in revised form 4 April 2019; Accepted 15 April 2019
Available online 19 April 2019

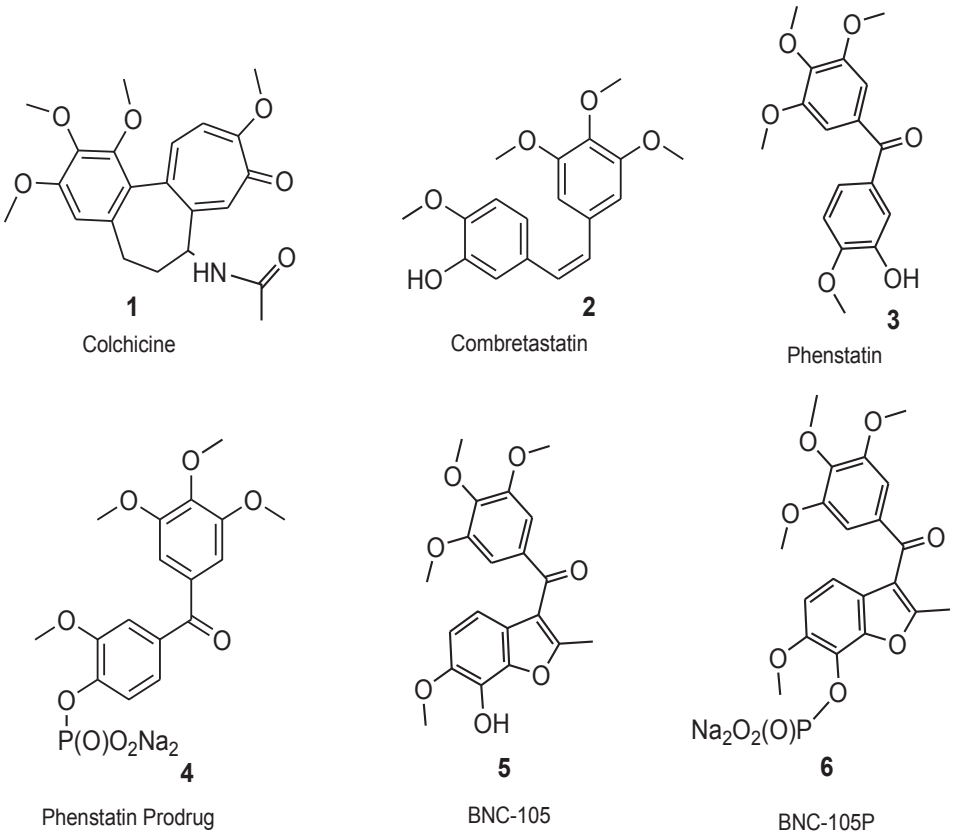

Fig. 1. Chemical structures of some established drugs (**2–6**) and clinical trials agents interacting with colchicine (**1**) binding site.

rapidly cleaved *in vivo* to the active agents [14,15]. A clinical study for BNC105P (**6**) has shown to be generally well tolerated [16,17]. It was found that the presence of both C7—OH and C2-substituents that sterically interact with the trimethoxybenzoyl (cisoid-coformer) in BNC105 structure are required for optimal potency of **5** as an anti-mitotic agent. The C7—OH group enables an additional hydrogen bonding interaction with Asn β258 to be achieved. Only when both effects are engendered (C7—OH + C2-substituent), the compound **5** exhibited good selectivity toward activated endothelial cells [16].

Heterocyclic benzo[*b*]furan is a structural unit of compounds with important pharmacological properties, including anticancer agents [18,19]. Both, naturally derived benzo[*b*]furans such as moracins [20,21], as well as synthetically obtained benzo[*b*]furan derivatives [22–27] bearing methoxy and/or hydroxy groups in their structures showed tubulin destabilizing activity. Herein, we report the synthesis and antiproliferative activity of 2-phenylbenzo[*b*]furan derivatives, functionalized with acetyl (**12b**), 3,4,5-trimethoxybenzoyl (**14**) and 4-hydroxy-3,5-dimethoxybenzoyl groups at 3-position (**13a, 13b**), as well as some 2-alkylbenzo[*b*]furan derivatives bearing bromine atom and functionalized with phenylacetyl substituent (**15, 16).** The compounds were evaluated against A375 melanoma cell line. The effects on tubulin polymerization, cell cycle and apoptosis were also evaluated. The aim of this study was established the influence of C4-OH substituent in the benzoyl group or phenyl group at C-2 position as well as an extra methylene between the carbonyl and phenyl group on the antiproliferative activities.

2. Results and discussion

2.1. Chemistry

2-Phenylbenzo[*b*]furan (**11a**) and 7-methoxy-2-phenybenzo[*b*]furans (**11b**) were obtained from 2-hydroxybenzaldehyde (**7a**) and 2-hydroxy-3-methoxybenzaldehyde (**7b**), correspondingly, through three stage synthesis (Scheme 1). *O*-Alkylation of the 2-hydroxybenzaldehydes with methyl 2-bromo-2-phenylacetate (**8**) in the presence of potassium bicarbonate in dimethylformamide gave the corresponding methyl 2-(2-formylphenoxy)-2-phenylacetates **9a** and **9b** in high yields. The desired 2-bromo-2-phenylacetate (**8**) was prepared in quantitative yield *via* sequential, one-pot process involves chlorination, bromination and esterification of phenylacetic acid. Hydrolysis of the methyl 2-(2-formylphenoxy)-2-phenylacetates (**9a** and **9b**) to the 2-(2-formylphenoxy)-2-phenylacetic acids (**10a** and **10b**), followed by cyclization of the acids gave benzo[*b*]furans **11a** and **11b** in good yields.

Studies on the environmental friendly method for acylation of 2-phenylbenzo[*b*]furans with acetic anhydride and 3,4,5-trimethoxybenzoic acid chloride with the use of ion-exchange Amberylst-15 resin as a catalyst were carried out. The optimal reaction conditions for the acetylation of 2-phenylbenzo[*b*]furan with acetic anhydride, using different ratio resin and acetic anhydride to the benzo[*b*]furans as well as different reaction time, were established. As result, 1-(2-phenylbenzo[*b*]furan-3-yl)ethan-1-one (**12a**) and 1-(7-methoxy-2-phenylbenzo[*b*]-furan-3-yl)ethan-1-one (**12b**) were obtained in highest yields (69–72%) when 2.5 equivalents of acetic anhydride to 1.0 equivalent of 2-phenylbenzo[*b*]furan and dry Amberlyst 15 resin were used and the reaction was carried out in anhydrous 1,2-dichloroethane under reflux for 6 h. The optimal reaction conditions for 7-methoxy-2-phenylbenzo[*b*]furan with 3,4,5-trimethoxybenzoic acid chloride were also established (1.1 equivalent of acid chloride, dry Amberlyst 15 resin and reaction times 6.5 h). The target 2-phenylbenzo[*b*]furan-3-yl)(3,4,5-trimethoxyphenyl)methanone (**14**) were obtained in good yield (69%) under these conditions.

A selective synthesis of (4-hydroxy-3,5-dimethoxyphenyl)-(2-phenylbenzo[*b*]furan-3-yl)methanone (**13a**) and (4-hydroxy-3,5-dimethoxyphenyl)(7-methoxy-2-phenylbenzo[*b*]furan-3-yl)-methanone (**13b**) was achieved by acylation of adequate 2-phenylbenozo[*b*]furan

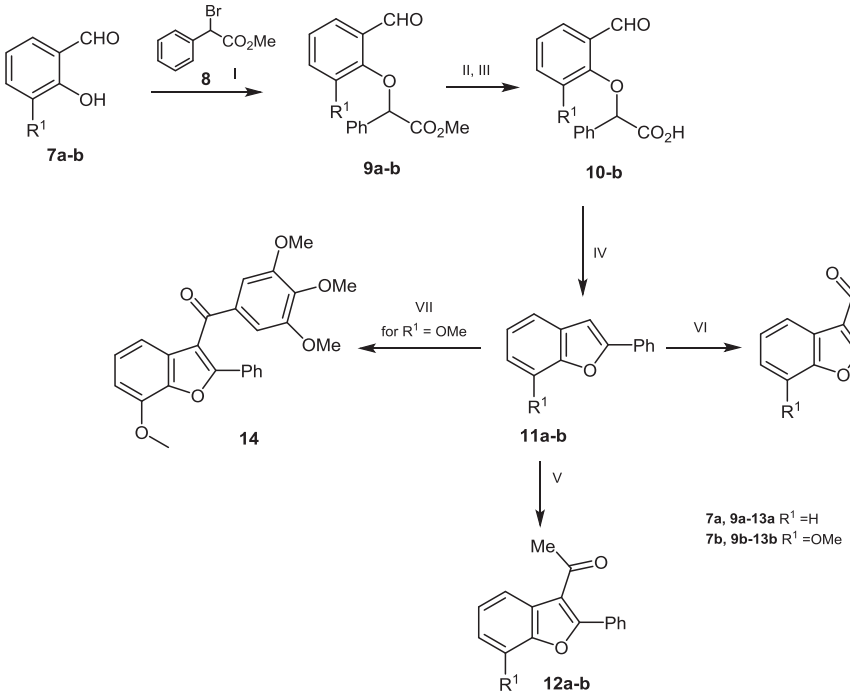

Scheme 1. Synthesis and acylation of 2-phenylbenzo[*b*]furans. *Reagents and conditions*: (I) **7** (1 equiv), K_2CO_3 (2 equiv), DMF, 92–94 °C, 4 h; (II) 10% aq KOH, 80 °C, 2.5 h; (III) 10% aq HCl, 0 °C to rt; (IV) Ac_2O, AcONa, 120–125 °C, 4 h, (V) 2-phenylbenzo[*b*]furan (1 equiv), acetic anhydride (2.5 equiv), dry Amberlyst 15 resin, 1,2-dichloroethane, reflux, 6.5 h (VI) 3,4,5-trimethoxybenzoyl chloride, $AlCl_3$ (3.0 equiv), 1,2-dichloroethane, 3.5 h, (VII) acid chloride (1,5 equiv), dry Amberlyst 15 resin, 1,2-dichloroethane, reflux, 6.5 h.

with 3,4,5-trimethoxybenzoyl chloride using an excess aluminium chloride catalyst to the 2-phenylbenzo[*b*]furan. When the reaction was carried out in 1,2-dichloroethane under reflux for 2–4 h the desired hydroxy product was obtained in yield of 68–76%.

The structural assignment of C4-OH group in **13a** and **13b** were achieved by comparative analysis of ^{1}H NMR spectra of adequate compounds. ^{1}H NMR spectra of compounds **11b, 12b, 13b** and **14** show the singlet peaks at 4.03, 4.09, 4.10 and 4.13 ppm, respectively that derived from the 3 protons of C-7 methoxy group; whereas the 6 protons derived from C-3 and C-5 methoxy group of **13a** and **13b** are observed at 3.71 and 3.92 ppm, respectively. Since in the structure of **13a** in position C7 is only aromatic proton, thus the ^{1}H NMR spectra unambiguously indicate for the selective demethylation of the C-4 methoxy group. The selective demethylation of C-4 methoxy group in 3,4,5-trimethoxyphenyl derivatives has been described in the literature [28,29].

To establish structure – proliferative activity relationship, 3-phenylcetyl functionalized 2-alkylbenzo[*b*]furans (**15** and **16)** were also prepared (Scheme 2). 1-(5-Bromo-2-ethylbenzo[*b*]furan-3-yl)-2-(4-hydroxyphenyl)ethanone (**15**) was obtained from 5-bromo-2-ethylbenzo[*b*]furan by acylation with 4-methoxyphenylacetyl chloride followed by demethylation of the methoxy group to hydroxy according to the procedure described previously [30]. 2-(3,5-Dibromo-4-hydroxyphenyl)-1-(2-butylbenzo[*b*]furan-3-yl)ethanone (**16**) was prepared from 2-butylbenzo[*b*]furan by sequential reactions: acylation with 4-methoxyphenylacetyl chloride, demethylation methoxy group and bromination, according to the procedure described previously [31,32].

2.2. Biological evaluation

2.2.1. In vitro antiproliferative activity

The antiproliferative activity of the compounds:**12b, 13a, 13b, 14, 15** and **16** was assessed using Cell Proliferation Reagent WST-1 assay. As shown in Table 1 and Fig. 2, assuming the benzo[*b*]furan inhibitory effects against A375 cells, the compounds **13a, 13b** and **14** revealed the highest antiproliferative activity, with IC_{50} values of 2.85 ± 0.82 μM, 0.86 ± 0.37 μM, 0.09 ± 0.03 μM, respectively. The obtained results showed low sensitivity of A375 cells to **12b, 15** and **16** compounds, with IC_{50} yielding > 100 μM.

2.2.2. Structure-activity relationships

The structure-activity relationship (SAR) was analysed with respect to the antiproliferative activity and IC_{50} value. Our data on 2-phenylbenzo[*b*]furans revealed that 3-aroyl group in 3 position is necessary to produce anticancer activity (**13a, 13b, 14**) since the analogue with 3-acetyl group (**12b**) was markedly less active (IC_{50} > 100 μM). Moreover, from three the most active 3-aroyl benzo[*b*]furan derivatives (**13a, 13b** and **14)** the most promising compound defined was **14** (IC_{50} = 0.09 ± 0.03 μM), with three methoxy group in the 3-aroyl substituent and 7-methoxy group on benzo[*b*]furan skeleton. It should be pointed that the differences between the three compounds become more distinct at 1 μM, where **13a** lost activity was seen (cell proliferation was equal to 95.79%, 54.36% and 10.51% for **13a, 13b** and **14**, respectively). This observation is in keeping with findings of Romagnoli et al. who indicated that antitumor activity of benzo[*b*]furan derivatives appeared to be dependent on substitution at the heterocyclic furan ring rather than at the benzene moiety [33]. Moreover, the replacement of the phenyl group at the 2-position to the alkyl group and introducing of an extra methylene between the carbonyl group and the phenyl group at the 3-position (compounds 15 and 16) caused a dramatic reduction in antiproliferative activity (IC_{50} > 100 μM) This can be explained by both reduction of the van der Waals forces after change phenyl to alkyl group and significant conformational changes after replacing of the rigid carbonyl-phenyl structure with carbonyl-methylene-phenyl structure.

Our findings are in line with other authors' observations, which emphasize the role of methoxy group in benzofuran anticancer activity. Moreover, Romagnoli et al. show that not only presence of a methoxy group but also its localization in benzo[*b*]furan skeleton is important. Namely, compounds with a methoxy substituent at the C-6 position of the benzofuran ring, exhibited the best antiproliferative activity in the 3-amino and 3-dimethylamino benzo[*b*]furan series, respectively, while shifting the methoxy group to the C-3, C-5 or C-7 position resulted in major loss in activity [34]. Romagnoli et al. revealed also that a methoxy group located at the C-6 position of the 2-(3′,4′,5′-trimethoxybenzoyl)-3-methylbenzo[*b*]furan derivative yields the most active compound, whereas changing its position to C-4, C-5 or C-7 lead to a reduction in potency [35].

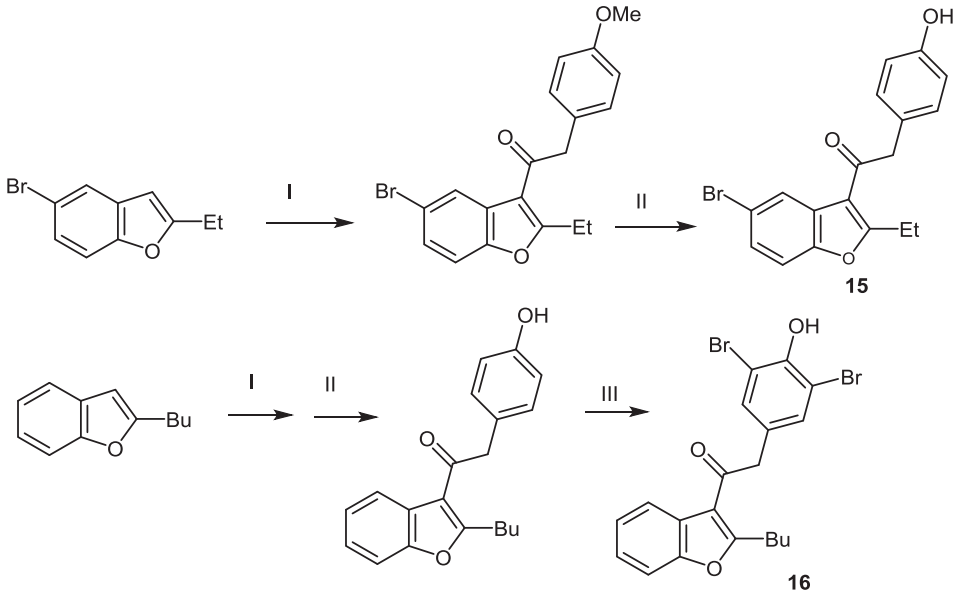

Scheme 2. Synthesis of **15** and **16.** Conditions: (I) 2-(4-methoxyphenyl)acetyl chloride (1 eq), $AlCl_3$ (1,5 eq), 1,2-dichloroethane, 0–15 °C, 6 h), (II) pyridine hydrochloride (10 eq), reflux, 10–12 min, (III) aq HBr (20%), $NaClO_3$, 3.6 eq, rt, 2 h [30–32].

Table 1
The IC_{50} (half maximal inhibitory concentration) values of benzo[*b*]furan derivatives against A375 cells, determined using WST-1 assay. The data indicate the mean of IC_{50} values (μM) ± SD of at least three independent experiments.

Compound	IC_{50} (μM)	Compound	IC_{50} (μM)
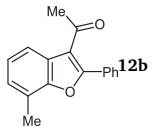 **12b**	> 100	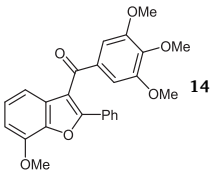 **14**	0.09 ± 0.03
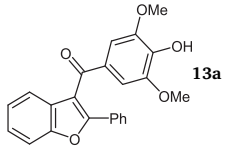 **13a**	2.85 ± 0.82	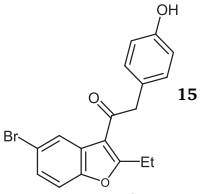 **15**	> 100
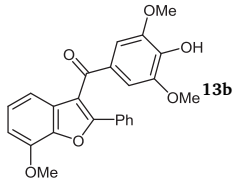 **13b**	0.86 ± 0.37	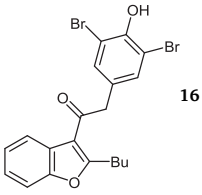 **16**	> 100

2.2.3. Cell morphology

Cytotoxicity of benzo[*b*]furan derivatives was also determined during cell culture optical microscopy imaging. The differences in A375 cells morphology were the most significant at the highest concentration of the tested compounds. As shown in Fig. 3 the cancer cells lost their characteristic shape and morphology, became spherical and ragged after treatment with **13a** and **13b** derivatives (100 μM) (Fig. 3C, D). It should be pointed that in **14** exposed cells (Fig. 3E) the similar effect was observed at even lower concentration 50 μM (**14** precipitates at higher concentration). As expected after exposure to less active **12b, 15** and **16** compounds only the cell density was lower, whereas cell morphology was preserved (Fig. 3B, F-G).

2.2.4. Apoptosis/necrosis detection – flow cytometry analysis

The FITC Annexin V Apoptosis Detection Kit II was used to detect apoptosis and necrosis of the cells after 48 h incubation with benzo[*b*]furan derivatives. Simultaneous staining with two dyes allows separation of four cell populations: viable (Annexin V-FITC− and PI−), early apoptotic state (Annexin V-FITC+ and PI−), late apoptotic or already dead (Annexin V-FITC+ and PI+) and necrotic (Annexin V-FITC− PI +). The flow cytometry analysis revealed negligible cytotoxicity of **12b, 15** and **16** - the percentage of live cells was high (about 90%) and comparable with the control. However, the late apoptosis level in **12b**, **15** and **16** treated cells was higher than in the control but did not exceed 8%. Simultaneously, high anticancer activity of 3-aroyl 2-phenylbenzo[*b*]furan derivatives was confirmed. Namely as shown in

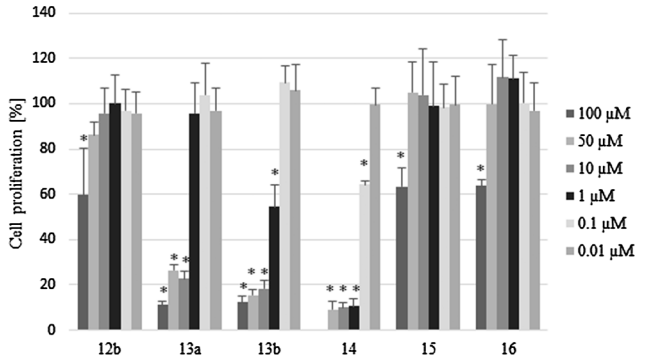

Fig. 2. The proliferation of A375 cells after 48 h exposure to the benzo[*b*]furan derivatives measured by WST-1 assay. *- $p < 0.05$ statistical significance between treated and control cells.

Fig. 4, after **13a, 13b** and **14** treatment, the percentage of late apoptotic cells increased to 57.63 ± 13.40%, 71.21 ± 15.03% and 58.52 ± 14.90%, respectively. Representative individual experiments are shown in Supplementary materials (Fig. S30).

2.2.5. Cell cycle analysis

As known tubulin destabilizing agents cause preferential G2–M blockade, therefore A375 cell populations were examined by flow cytometry to quantify cellular DNA content and cell cycle distribution. As expected 3-aroyl 2-phenylbenzo[*b*]furan compounds caused accumulation of A375 in a tetraploid (4 N) state decreasing the percentage of cells in G0/G1 phase (Fig. 5). The percentage of A375 cells in G2/M phase was 66.34 ± 3.26%, 58.86 ± 5.11%, 63.62 ± 9.16% for **13a** (100 μM), **13b** (100 μM) and **14** (50 μM), respectively. In contrast, after exposure to compounds **12b** (100 μM), **15** (100 μM) and **16** (100 μM) percentage of A375 cells in G0/G1 and G2/M phase was comparable and similar to the control (untreated) cells. Our data are in line with Kamal et al. data showing G2/M cell cycle arrest as common mechanism leading to cancer cell apoptosis after benzofuran treatment [36].

2.2.6. Confocal microscopy imaging

To confirm that the aforementioned cell cycle arrest is related to an interaction with the microtubule system a confocal microscopy analysis was performed. After 7 h-incubation of the cells with the tested compounds, the cells were fixed and α-tubulin and chromosomes were stained. The control cells in mitosis showed bipolar spindle formation with chromosomes arrangement in the central metaphase plate or anaphase distribution (Fig. 6A, B). Similarly, after **12b** treatment most of dividing cells were regular (single uncommon mitosis was presented at Fig. S32(A, B). However, in 3-aroyl 2-phenylbenzo[*b*]furans treatment cells different phenotypes with enormous nuclei, diffused chromosomes and no mitotic spindle were observed (Fig. 6 C–H). Especially, in **14** binuclear or huge nuclei are common. Additional graphs with scale are presented in Supplementary materials (Fig. S31). In **15** and **16** treated cells normal bipolar spindles and single abnormal spindles (with monoastral, tangled microtubules, diffused chromosomes or two asymmetric asters close to each other) were detected. Examples of abnormal spindles detected in **15** and **16** treated cells are shown in Fig. S32(C-F).

The differences between cells treated with the tested compounds and untreated are noticeable only during mitosis, suggesting mitotic-specific activity of the compounds. Our data are in contrary to Kamal et al. study, where the most active compounds: (6-methoxy-5-((4-methoxyphenyl)ethynyl)-3-methylbenzo[*b*]furan-2-yl)(3,4,5trimethoxyphenyl)methanone and (*E*)-3-(6-methoxy-3-methyl-2-(1-(3,4,5-trimethoxyphenyl)vinyl)benzo[*b*]furan-5-yl)prop-2-en-1-ol disrupted microtubule organization in all cells [36]. Cell-permeable small molecules that perturb mitosis without effects on microtubule/cytoskeleton in interphase may be useful in anticancer therapy and contribute to decrease in side effects.

2.2.7. Cell free tubulin polymerization assay

The effects of benzo[*b*]furan derivatives on tubulin polymerization in cell free conditions were evaluated using a fluorescence-based tubulin polymerization assay. The activity of the tested compounds was compared with paclitaxel (PTX), vinblastine (VBL) and 0.2% DMSO as the control and reference. As shown in Fig. 7, DMSO in the control sample had no direct effect on tubulin polymerization and generated three typical phases of spontaneous microtubule formation, namely nucleation, growth and steady state inhibition. The references compounds, like PTX and VBL, interacted with tubulin, and altered normal polymerization curve. The overlapping VBL, **13a, 13b** (100 μM) and **14** (50 μM) curves confirm that these three the most active compounds, inhibit tubulin polymerization causing decrease in V_{max} (maximal slope values for the growth phase) and reduction in final polymer mass protein. These data are in line with confocal microscopy imaging and flow cytometry analysis, since inhibition of tubulin polymerization prevent mitotic spindle formation leading to polyploidy nuclei and cell cycle arrest in 4 N. In comparison with these compounds **15** and **16** showed moderate impact on microtubule formation. Because of high auto-florescent signal of compound **12b**, it was not evaluated in the fluorescence based tubulin polymerization assay.

3. Conclusion

We described efficient synthesis of 2-phenylbenzo[*b*]furans *via* corresponding 2-(2-formylphenoxy)-2-phenylacetic acids and their functionalization at 3-positon. 3-Acetyl and 3-trimethoxybenzoyl derivatives of 2-phenylbenzo[*b*]furan can be obtained in good yields by a selective, green acylation method with the use of Amberlyst 15 ion exchange resin as a catalyst. The reaction conditions for selective synthesis of (4-hydroxy-3,5-dimethoxyphenyl)(2-phenylbenzo[*b*]furan-3-yl)methanones were also presented. The functionalized benzo[*b*]furans as well as other 3-acylated 2-alkylbenzo[*b*]furans were evaluated as antitumor agents.

Among the tested compounds, 2-phenyl derivatives **13a** and **13b** containing 4-hydroxy-3,5-dimethoxybenzoyl group as well as **14** bearing 3,4,5-trimethoxybenzoyl group exhibited the most potent antiproliferative activity against human melanoma A375 cell line. The change of the phenyl substituent with alkyl at C2-furan ring as well as introducing of an extra methylene between the carbonyl and the phenyl group at the 3-position caused a dramatic reduction in antiproliferative activity. It was also found that 7-methoxy group in 2-phenylbenzo[*b*]furan skeleton contribute to increase anticancer activity. Tubulin polymerization assay, confocal microscopy imaging and flow cytometry analysis revealed that 3-aroyl-2-phenylbenzo[*b*]furans inhibited tubulin polymerization leading to disruption of mitotic spindle formation, cell cycle arrest in G2/M phase and apoptosis. Further studies to develop synthesis and antiproliferative activity evaluation for the 3-functionalized 2-arylbenzo[*b*]furan derivatives including these containing the 7-hydroxy group are in progress in our laboratory and will be reported in due course.

4. Experimental section

4.1. Chemistry

4.1.1. General

NMR spectra were recorded with TM Bruker DPX-400 (400 MHz) spectrometer. Chemical shifts (δ) are given in ppm from TMS (0 ppm), as an internal standard for ^{1}H NMR, and $CDCl_3$ (77.0 ppm), for ^{13}C NMR (100 MHz). Coupling constants (*J*) in hertz (Hz). Abbreviations are as follows: s (singlet), d (doublet), t (triplet), q (quartet), m (multiplet), br

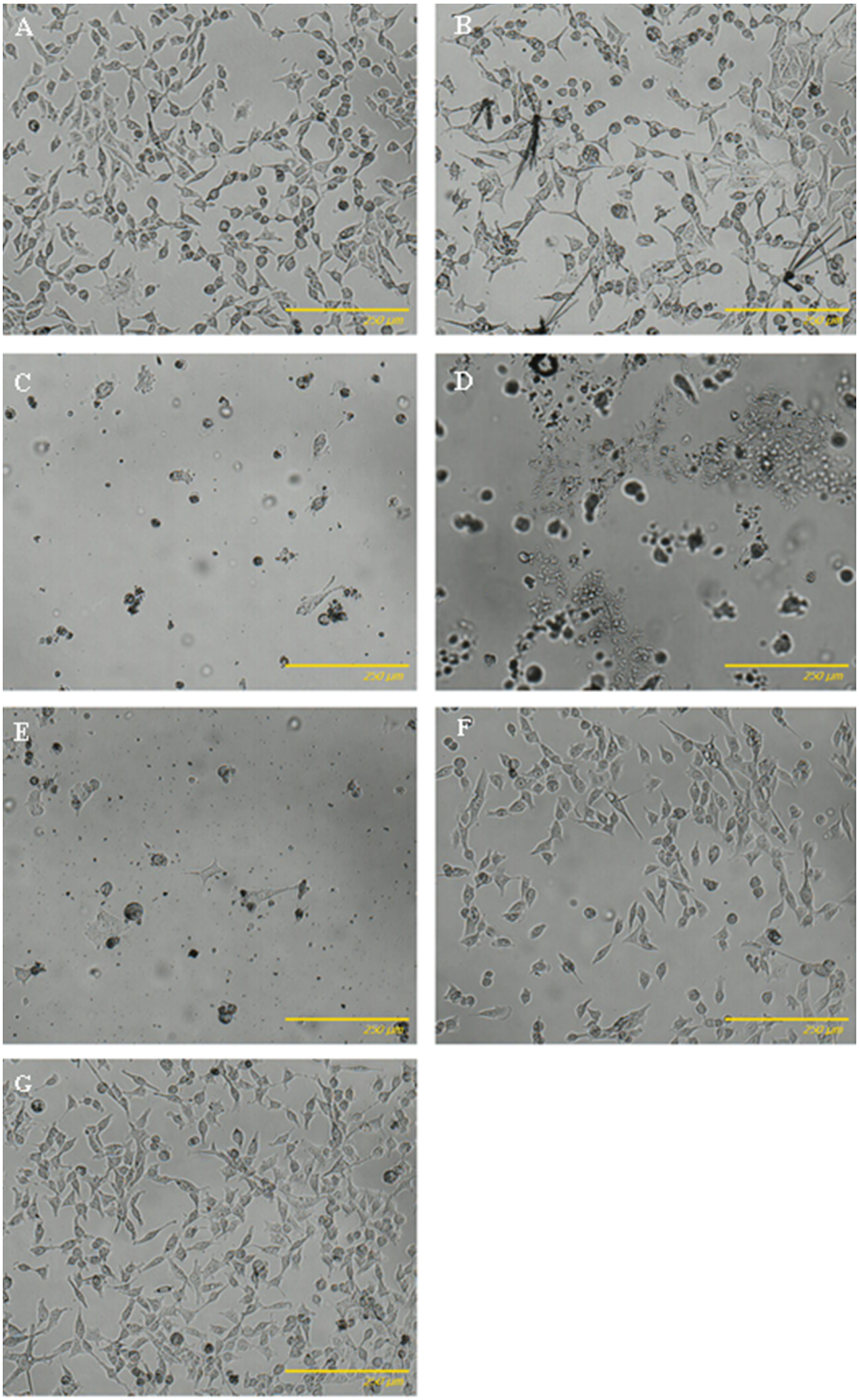

Fig. 3. Optical microscopy images of A375 cells, controls (A) and after 48 h incubation with 100 μM of compounds: **12b** (B), **13a** (C), **13b** (D), **15** (F), **16** (G); 50 μM of **14** (E).

(broad).

GC/MS analysis were performed using an Agilent Technologies 6890 N apparatus, equipped with a mass detector 5973 Network and 3.0 m × 0.25 mm capillary column, filled with a 0.25-μm film of 5% MePh silicate. Injector temperature was 250 °C. A gradient of temperature was 60 °C for 3 min., then an increase of 10 °C/min., to 300 °C.

Fourier transform infrared-attenuated total reflection spectroscopy (FTIR–ATR) was performed using a Nexus spectrometer with Golden Gate (ATR) (Thermo Nicolet Corp.). Samples were dried at 60 °C under vacuum for 24 h, and 32 scans were averaged across the spectral range of 400–4000 cm^{-1}. All melting points were determined using a Boetius apparatus and are uncorrected.

Most of the reagents and solvents were purchased in commercially available grade purity. 1,2-Dichloroethane was dried with calcium

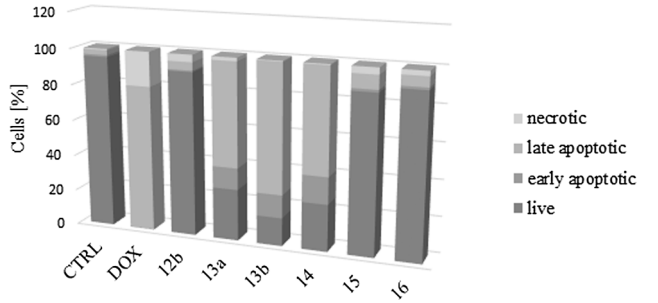

Fig. 4. The effect of benzo[*b*]furan derivatives (at concentration of 100 μM, except for **14**: 50 μM) on the induction of apoptosis in A375 cells after 48 h treatment. The population of live and apoptotic/necrotic cells was determined using flow cytometry. Two controls were included: untreated cells growing in medium with DMSO (negative control) and treated with doxorubicine 11.41 μM (positive control). Means of at least three independent experiments are shown.

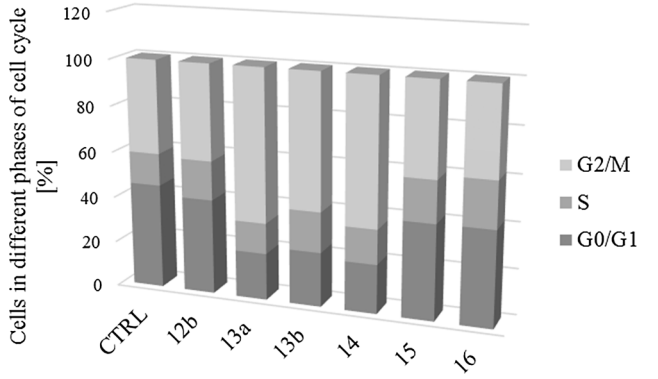

Fig. 5. Flow cytometric analysis of A375 cells cycle using Orange dye staining after exposure to benzo[*b*]furan derivatives for 7 h (means of at least two independent experiments are shown).

hydride before the use. Commercially Amberlyst 15 was dried before the use by azeotropic evaporation of water with chloroform.

Methyl 2-bromo-2-phenylacetate **8** was obtained from phenylacetic acid by sequential processes chlorination, bromination and esterification (Supporting materials) although it is commercially available.

*4.1.2. General procedure for synthesis of compounds **9a** and **9b***

A mixture of methyl 2-bromo-2-phenylacetate (**8**) (10.8 g, 47 mmol), 2-hydroxybnezaldehyde **7a** or **7b** (47 mmol), K_2CO_3 (7.6 g, 55 mmol) and DMF (100 mL) was stirred and heated at 92–94 °C for 4.5 h. Then, the mixture was cooled, poured onto ice/H_2O (150 mL) and the mixture left to stand at 4 °C for 12 h. After this, the precipitate was filtered off, washed with H_2O and dried to give crude product as a solid.

*4.1.2.1. Methyl 2-(2-formylphenoxy)-2-phenylacetate (**9a**).* Yield: 9.8 g (76%); a pale brown solid; mp. 103–105 °C; GC/MS τ = 19.84, MS *m/z* (%) 270 (M^+, 13), 238 (21), 211 (51), 194 (40), 181 (49), 165 (48), 152 (13), 133 (100), 121 (29), 105 (57), 89 (14), 77 (62), 59 (13), 51 (19).

*4.1.2.2. Methyl 2-(2-formyl-6-methoxyphenoxy)-2-phenylacetate (**9b**).* Yield: 4.01 g (60.7%); a pale beige solid; mp 79–82 °C; GC/MS τ = 21.48, MS *m/z* (%) 300 (M^+, 56) 240 (52),224 (35), 211 (54), 197 (36), 181 (37), 167 (15), 163 (100),151 (48), 141 (17), 121 (20), 105 (39), 89 (14), 77 (54), 59 (23), 51 (17). ^{1}H NMR (400 MHz, $CDCl_3$) δ 10.50 (s, 1H, CHO), 7.53–7.48 (m, 2H, 2xAr-CH), 7.43–7.35 (m, 4H, 4xAr-CH), 7.17–7.09 (m, 2H, 2xAr-CH), 5.93 (s, 1H, CH), 3.90 (s, 3H, OCH_3), 3.72 (s, 3H, OCH_3). ^{13}C NMR (101 MHz, $CDCl_3$) δ 190.6, 170.4, 151.9, 149.1, 135.3, 130.0, 129.4, 128.9, 127.6, 124.4, 121.4, 119.2, 117.9, 82.0, 56.2, 52.4.

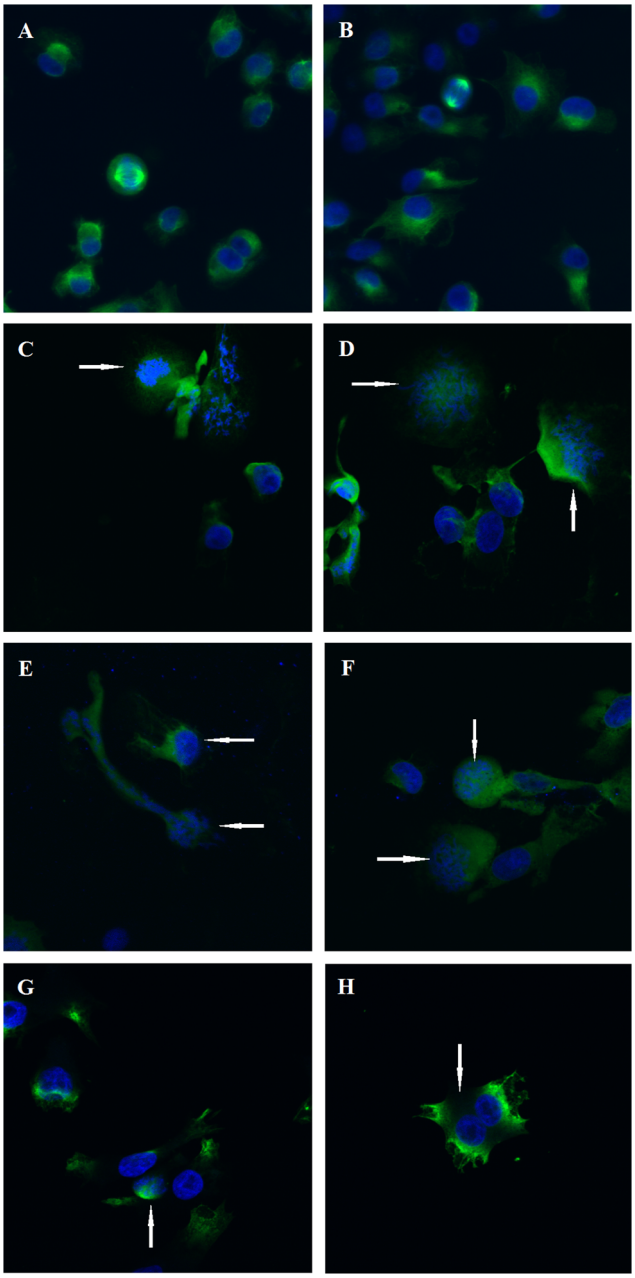

Fig. 6. Confocal microscopy imaging of A375 cells: the control (A, B) and after 7 h incubation with compound **13a** (C, D), **13b** (E, F) at concentration of 100 μM and **14** (G, H) at 10 μM, with stained α-tubulin (green) and chromosomes (blue); magnification 400×. Abnormal spindles were marked with arrows.

*4.1.3. General procedure for synthesis of compounds **10a** and **10b***

A mixture of methyl 2-(2-formylphenoxy)-2-phenylacetate (**9a** or **9b**) (7 mmol) 10% aq KOH (30 mL) and methanol (2 mL) was stirred and heated at 75–80 °C for 2 h. After the mixture was cooled to rt, 10% aq HCl was added under stirring and cooling with ice. The precipitate was filtered off, washed several times with H_2O and dried. The crude product was obtained as a solid.

*4.1.3.1. 2-(2-Formylphenoxy)-2-phenylacetic acid (**10a**).* Yield (70%); white solid, mp 140–141 °C, lit. 140–142 °C [37]; Anal. Calcd for $C_{15}H_{12}O_4$: C, 70.31; H, 4.72. Found: C, 70.18; H, 4.92.

*4.1.3.2. 2-(2-Formyl-6-methoxyphenoxy)-2-phenylacetic acid (**10b**).* Yield: 2.3 g (72%); a pale beige solid mp 55–56 °C. ^{1}H NMR (400 MHz, $CDCl_3$)

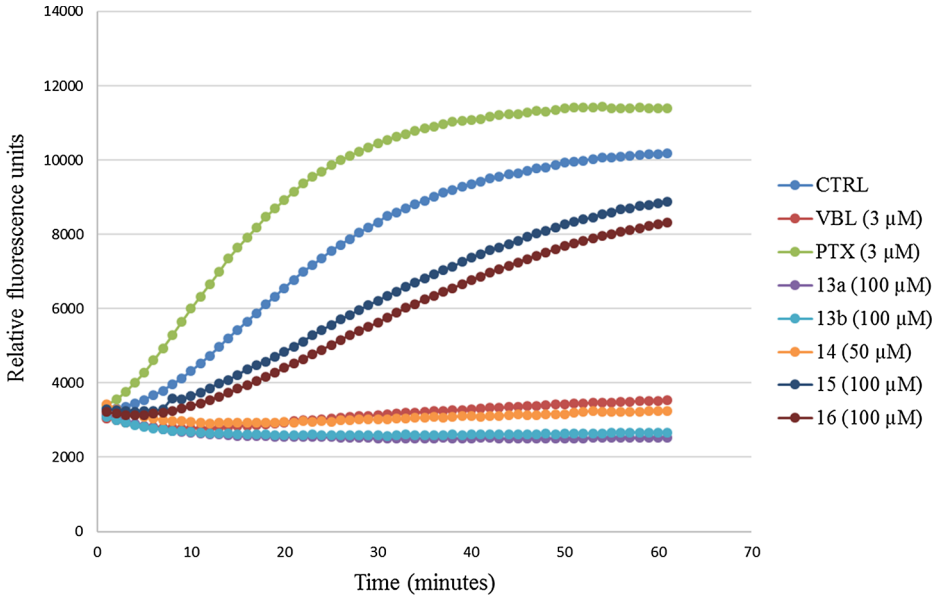

Fig. 7. Effects of benzo[*b*]furan derivatives on tubulin polymerization in cell free conditions. Paclitaxel (PTX) and vinblastine (VBL) were used as references and DMSO as a vehicle control. The final DMSO concentration did not exceed 0.2% in all samples. Means of at least three independent experiments are shown.

δ 10.27 (s, 1H, CHO), 7.50–7.43 (m, 2H, Ar), 7.40–7.31 (m, 4H, Ar), 7.19–7.09 (m, 2H, Ar), 6.51 (bs, 1H, COOH), 5.93 (s, 1H, CH), 3.85 (s, 3H, OCH_3). ^{13}C NMR (101 MHz, $CDCl_3$) δ 191.5, 173.6, 151.8, 148.1, 134.8, 129.6, 129.5, 129.0, 127.8, 124.7, 121.2, 118.3, 82.2, 56.1.

*4.1.4. General procedure for synthesis of compounds **11a** and **11b***

A mixture of 2-(2-formylphenoxy)-2-phenylacetic acid (**10a** or **10b**) (3.3 mmol), anhydrous AcONa (33 mmol, 10 equiv) and Ac_2O (35 mL) was stirred and heated at 125–130 °C for 4.5 h. Then, the mixture was cooled and poured onto ice/H_2O (130 mL) and left at refrigerator for 12 h. The precipitate was filtered off, washed several times with cooled H_2O and dried. The crude product was recrystallized from *n*-hexane.

*4.1.4.1. 2-Phenylbenzo[b]furan (**11a**).* Yield: 90%; a pale beige solid, mp 112–115 °C; GC/MS τ = 17.14 min, MS *m/z* (%) 194 (M^+, 100), 165 (63), 139 (10), 126 (3%), 115 (5%), 97 (5%), 77 (4%), 63 (9), 51 (6%).

^{1}H NMR (400 MHz, $CDCl_3$) δ 7.87 (dt, J = 3.0, 1.7 Hz, 2H, Ar), 7.61–7.56 (m, 1H, Ar), 7.56–7.50 (m, 1H, Ar), 7.48–7.42 (m, 2H, Ar), 7.39–7.32 (m, 1H, Ar), 7.31–7.20 (m, 2H, Ar), 7.03 (d, J = 0.8 Hz, 1H, CH (furan). ^{13}C NMR (101 MHz, $CDCl_3$) δ 155.9, 154.9, 130.5, 129.2, 128.8, 128.5, 124.9, 124.2, 122.9, 120.9, 111.2, 101.3.

*4.1.4.2. 7-Methoxy-2-phenylbenzo[b]furan (**11b**).* Yield: 1.21 g (96.8%); a pale beige solid; mp 65–68 °C. GC/MS τ = 19.66 min, MS *m/z* (%) 224 (M^+, 100), 181 (30), 153 (40), 152 (50), 127 (8), 112 (4), 102 (4), 87 (3), 76 (7), 63 (4), 51 (5). ^{1}H NMR (400 MHz, $CDCl_3$) δ 7.91–7.86 (m, 2H, Ar), 7.46–7.39 (m, 2H, Ar), 7.36–7.30 (m, 1H, Ar), 7.20–7.11 (m, 2H, Ar), 7.00 (s, 1H, CH, furan), 6.79 (dd, J = 7.4, 1.4 Hz, 1H, Ar), 4.03 (s, 3H, OCH_3). ^{13}C NMR (101 MHz, $CDCl_3$) δ 156.0, 145.3, 144.1, 130.9, 130.3, 128.7, 128.5, 125.0, 123.6, 113.3, 106.7, 101.6, 56.1.

*4.1.5. General procedure for synthesis **12a-b***

A mixture of benzo[*b*]furan (**11a** or **11b**) (22 mmol) Ac_2O (0.3 mL, 33 mmol, 1.5 equiv), Amberlyst 15 (1 g) and 1,2-dichloroethane (20 mL) was stirred at reflux for 6 h. The catalyst was filtered, the filtrate neutralized by 5% aq sodium hydroxide. The organic layer was separated and solvent removed. The crude product was recrystallized from *n*-hexane.

*4.1.5.1. 1-(2-Phenylbenzo[b]furan-3-yl)ethan-1-one (**12a**) Yield: 69%, a semi-solid.* ^{1}H NMR (400 MHz, $CDCl_3$) δ 8.15–8.07 (m, 1H, Ar-CH), 7.77–7.71 (m, 2H, Ar), 7.54–7.48 (m, 4H, Ar), 7.38–7.32 (m, 2H, Ar), 2.37 (s, 3H, $COCH_3$). ^{13}C NMR (101 MHz, $CDCl_3$) δ 195.6, 160.5, 154.0, 130.6, 130.2, 129.8, 128.7, 126.9, 125.5, 124.4, 122.5, 118.5, 111.2, 30.6.

*4.1.5.2. 1-(7-Methoxy-2-phenylbenzo[b]furan-3-yl)ethan-1-one (**12b**).* Yield (72%), a pale brown solid; mp. 118–121 °C. GC/MS τ = 23.62 min, MS *m/z* (%) 266 (M^+, 58), 251 (100), 223 (12), 165 (22), 152 (26), 126 (8), 102 (5), 76 (4), 51 (2). ^{1}H NMR (400 MHz, $CDCl_3$) δ 7.94–7.92 (m, 2H), 7.83 (s, 1H), 7.77 (d, J = 8.44 Hz, 1H), 7.45 (t, J = 7.45, 2H), 7.39–7.36 (m, 1H), 6.78 (d, J = 8.43 Hz, 1H), 4.09 (s, 3H, OCH_3), 2.63 (s, 3H, $COCH_3$). ^{13}C NMR (400 MHz, $CDCl_3$) ^{13}C NMR (400 MHz, $CDCl_3$) δ 197.3, 158.1, 148.9, 143.9, 130.5, 129.8, 129.0, 128.8, 127.9, 125.2, 123.1, 105.5, 103.3, 56.3, 27.0. IR (KBr) ν_{max}/cm^{-1} 1654, 1620, 1573.

*4.1.6. General procedure for synthesis of compounds **13a** and **13b***

To a stirring mixture of benzo[*b*]furan (**11a** or **11b**) (22 mmol), 3,4,5-trimethoxybenzoyl chloride (0.5 g, 2.2 mmol) and dry 1,2-dichloroethane (30 mL) was added $AlCl_3$ (0.88 g, 6.6 mmol, 3 equiv) in portion, at 45 °C for 1 h. The heating was continued at 45–50 °C for 2.5 h. The mixture was cooled to rt and poured into solution of ice/water (20 mL) and 35% HCl (1 mL) and the layers was separated. Organic layer was washed with water (2 × 15 mL), 2% aq NaOH (2 × 15 mL) and water (2 × 15 mL). The organic layer was dried (Na_2SO_4)separated and solvent removed under vacuo. The crude product was recrystallized from *n*-hexane.

*4.1.6.1. (4-Hydroxy-3,5-dimethoxyphenyl)(2-phenylbenzo[b]furan-3-yl) methanone (**13a**).* Yield: 68%, a dark beige solid mp 107–109 °C. GC/MS τ = 28,99 min, MS *m/z* (%) 374 (M^+, 100), 359 (10), 343 (12), 271 (10), 241 (10) 221 (47), 181 (23), 165 (55), 139 (15), 123 (10), 108 (6), 67 (8), 53 (3). ^{1}H NMR (400 MHz, $CDCl_3$) δ 7.74–7.65 (m, 3H, Ar), 7.60–7.57 (m, 1H, Ar), 7.39–7.22 (m, 5H, Ar), 7.19 (s, 2H, Ar), 6.0 (1H, OH), 3.71 (6H, OCH_3). ^{13}C NMR (101 MHz, $CDCl_3$) δ 190.5, 156.8, 154, 146.8, 139.9, 129.8, 129.7, 128.7, 128.6, 128.4, 125.5, 123.9, 121.6, 116.0, 111.3, 107.5, 56.4, 43.6. IR (KBr) ν_{max}/cm^{-1} 3367, 1638, 1602, 1579.

*4.1.6.2. (4-Hydroxy-3,5-dimethoxyphenyl)(7-methoxy2-phenylbenzo[b] furan-3-yl)methanone (**13b**).* Yield: 76%, a dark beige solid mp

67–69 °C. ^{1}H NMR (400 MHz, $CDCl_3$) δ 7.92 (dd, J = 5.2, 3.4 Hz, 2H, Ar), 7.59 (d, J = 8.4 Hz, 1H, Ar), 7.49 (s, 1H, Ar), 7.48–7.41 (m, 2H, Ar), 7.40–7.34 (m, 1H, Ar), 7.15 (s, 2H, Ar), 6.82 (d, J = 8.4 Hz, 1H, Ar), 6.05 (bs, 1H, OH), 4.10 (s, 3H, OCH_3), 3.91 (s, 6H, OCH_3). ^{13}C NMR (101 MHz, $CDCl_3$) δ 194.9, 157.8, 148.4, 146.6, 144.1, 138.8, 131.8, 130.0, 129.8, 129.1, 128.8, 128.8, 125.3, 123.2, 107.5, 105.4, 102.6, 56.5, 56.3. IR (KBr) ν_{max}/cm^{-1} 3351, 1638, 1613, 1579.

4.1.7. Synthesis of (7-Methoxy-2-phenylbenzo[b]furan-3-yl)(3,4,5-trimethoxyphenyl) methanone (14)

A mixture of benzo[*b*]furan (**11b**) (0.5 g, 2.2 mmol), 3,4,5-trimethoxybenzoyl chloride (0.5 g, 2.2 mmol), Amberlyst 15 (0.3 g) and1,2-dichloroethane (20 mL) was stirred at reflux for 6.5 h. The catalyst was filtered, the filtrate neutralized by 5% aq sodium hydroxide. The organic layer was separated, dried ((Na_2SO_4) and solvent removed under vacuo. The crude product was recrystallized from *n*-hexane.

Yield: 69%; a pale brown solid mp 64–66; GC/MS, τ = 34.9 min, MS *m/z* (%) 418.2 (M^+, 100), 387.1 (10), 375.1 (15), 251.1 (60), 165 (15), 152 (15). ^{1}H NMR (400 MHz, $CDCl_3$) δ 7.93 (dd, J = 5.2, 3.4 Hz, 2H, Ar), 7.61 (d, J = 8.4 Hz, 1H, Ar), 7.57 (s, 1H, Ar), 7.50–7.43 (m, 2H, Ar), 7.41–7.34 (m, 1H, Ar), 7.09 (s, 2H, Ar), 6.81 (d, J = 8.4 Hz, 1H, Ar), 4.13 (s, 3H, OCH_3), 3.96 (s, 3H, OCH_3), 3.89 (s, 6H, 2xOCH_3). ^{13}C NMR (101 MHz, $CDCl_3$) δ 194.5, 158.0, 152.9, 148.6, 144.1, 141.5, 134.2, 131.9, 129.8, 129.3, 129.1, 128.8, 125.4, 122.8, 107.4, 105.4, 102.7, 61.0, 56.4, 56.3. IR (KBr) ν_{max}/cm^{-1} 1638, 16013, 1573.

4.1.8. 1-(5-Bromo-2-ethylbenzo[b]furan-3-yl)-2-(4-hydroxyphenyl) ethanone (15)

A white solid, mp 144–146 °C, ^{1}H NMR (400 MHz, $CDCl_3$/DMSO-d_6) δ 8.95 (s, 1H, OH), 8.14 (s, 1H, Ar), 7.49–7.27 (m, 2H, Ar), 7.03 (d, J = 8.4 Hz, 2H, Ar), 6.79 (d, J = 8.4 Hz, 2H, Ar), 4.15 (s, 2H, CH_2), 3.17 (q, J = 7.5 Hz, 2H, CH_2), 1.35 (t, J = 7.5 Hz, 3H, CH_3).

^{13}C NMR (101 MHz, $CDCl_3$/DMSO-d_6) δ 194.0, 168.3, 156.3, 152.1, 130.4, 128.0, 127.2, 124.4, 124.0, 116.9, 115.8, 115.5, 112.5, 48.2, 22.5, 11.9.

4.1.9. 2-(3,5-Dibromo-4-hydroxyphenyl)-1-(2-butylbenzo[b]furan-3-yl) ethanone (16)

A white solid mp, 107–109 °C; ^{1}H NMR (400 MHz, $CDCl_3$) δ 7.92–7.85 (m, 1H, Ar), 7.53–7.46 (m, 1H, Ar), 7.38–7.29 (m, 4H, Ar), 5.94 (bs, 1H, OH), 4.19 (s, 2H, CH_2), 3.20–3.11 (m, 2H, CH_2), 1.76 (dt, J = 12.8, 7.6 Hz, 2H, CH_2), 1.49–1.35 (m, 2H, CH_2), 0.95 (t, J = 7.4 Hz, 3H, CH_3). ^{13}C NMR (101 MHz, $CDCl_3$) δ 193.0, 167.9, 153.7, 148.5, 133.3, 128.4, 125.4, 124.6, 124.1, 121.1, 116.2, 111.4, 109.8, 47.6, 29.9, 28.8, 22.6, 13.8.

4.2. Biological evaluation

4.2.1. Cell culture

Human malignant melanoma cells (A375, catalogue no. 88113005) were purchased from European Collection of Authenticated Cell Cultures (ECACC). Cells were cultured in a humidified incubator (5% CO_2, 37 °C) in culture medium (Dulbecco's Modified Eagle Medium, Sigma-Aldrich, Germany) supplemented with glucose (4.5 g/L), sodium pyruvate (0.11 g/L), 10% heat-inactivated fetal bovine serum (HyClone, South America), L-glutamine (2 mM, Sigma-Aldrich, Germany) and 0.4% penicillin-streptomycin (Sigma-Aldrich, Germany).

4.2.2. Antiproliferative activity and cell morphology

The antiproliferative activity of the compounds was evaluated using the Cell Proliferation Reagent WST-1 assay (Sigma-Aldrich, Germany). The WST-1 test is based on the reduction of the tetrazolium salt WST-1 to a soluble red formazan by mitochondrial dehydrogenase. The amount of formazan dye is directly correlated to the number of metabolically active cells. In the present study, A375 cells were seeded in 96-well plate (2×10^3 cells/well) and then cultured in 100 μL medium in standard conditions. After 24 h the culture medium was removed and the cells were treated with tested compounds at final concentrations in the medium: 0.01, 0.1, 1, 10, 50, 100 μM for 48 h. All the tested compounds were dissolved in DMSO. In the final concentrations the amount of DMSO did not exceed 0.2%. The cells without the tested compounds were used as the controls. After 48 h cell morphology was recorded using Smart Fluorescent Cell Analyzer Microscope JuLi™ (Korea). Next the WST-1 reagent was added (10 μL), incubated with the cells for 30 min and then the absorbance was measured at 450 nm (with 620 nm background correction), using a spectrophotometric microplate reader (Infinite 200 Pro, Tecan, Switzerland). The interaction between compounds (without cells) and WST-1 reagents was also determined (Ablank). The results were normalized to the control cells, and the cell viability was calculated using the following formula: number of viable cells (% of control) = [(Atest − Ablank)/(Acontrol − Ablank)] × 100%. The readings were acquired from three independent experiments (each conducted in triplicate). For the most active compounds (**13a**, **13b**, **14**) three additional WST-1 experiments (each conducted in triplicate) with additional dilution factors (10; 5; 1; 0.5; 0.1; 0.05; 0.01 μM) were performed. Statistical analysis was carried out using Statistica 12 (StatSoft Inc., Tulsa, Oklahoma, USA). Results are expressed as mean ± standard deviation. Experimental data were assessed using the Student's *t*-test. A p-value level of < 0.05 was considered statistically significant.

4.2.3. Apoptosis/necrosis detection - flow cytometry analysis

FITC Annexin V Apoptosis Detection Kit II (BD Pharmingen, Belgium) was used to distinguish apoptotic and necrotic cells after tested compounds treatment. A375 cells were plated in 6-well plates (5×10^4 cells/well). After 24 h the culture medium was removed and the cells were treated with tested compounds at final concentrations of 100 μM, except for **14** (50 μM) and incubated for another 48 h. After treatment the cells were washed with PBS (both the cell medium and PBS were collected) and harvested by trypsinization. After centrifugation, the supernatant was discarded, the cells were washed with PBS and again spin. After centrifugation, the supernatant was discarded, pellet was resuspended in 1X Binding Buffer and incubated with Annexin V-FITC and propidium iodide (PI) for 15 min at room temperature in the dark. Next, stained A375 cells were diluted by 1X Binding Buffer and directly analyzed by Navios flow cytometer (Beckman Coulter, USA). The positive Annexin V-FITC indicates the loss of plasma membrane, which characterizes the early stage of apoptosis. The positive PI indicates the damage of cell membrane, which occurs either in the terminal stage of cell apoptosis or necrosis. Therefore, the apoptotic cells were identified as Annexin V-FITC+ and PI−, the nonviable cells were identified as Annexin V-FITC+ and PI+, and the viable cells as Annexin V-FITC− and PI−. Two controls were used: untreated cells growing in medium with DMSO (negative control) and treated with doxorubicine 11.41 μM (positive control). The readings were acquired from three independent experiments.

4.2.4. Cell cycle analysis

For cell cycle analysis, A375 cells were seeded in 12-well plates (2×10^4 cells/well), cultured for about 41 h and next additional 7 h [38] with 100 μM of the compounds: **12b, 13a, 13b, 15, 16** and 50 μM of compound **14**. Next, medium was collected, cells were washed with PBS and collected by trypsynization. After centrifugation, supernatant was discarded and pellet was resuspended in medium (1 mL) with Vybrant® DyeCycle™ Orange Stain (10 μM, Thermofishern Scientific), incubated for 30 min at 37 °C, and DNA content was measured by Navios flow cytometer (Beckman Coulter, USA). The cell proportions in G0/G1, S and G2/M phases were analyzed using an appropriate software (Kaluza Flow Cytometry Analysis Software, Beckman Coulter, ModFit LT 4.1, Verity Software House, USA). The readings were acquired from three independent experiments.

4.2.5. Confocal microscopy imaging

To visualize the microtubule and DNA, A375 cells were seeded on coverslips at density of 5×10^4 cells, and cultured as above for about 41 h. Afterwards, 100 μM of the compounds: **12b, 13a, 13b, 15, 16** and 10 μM of compound **14** were added, and incubated for additional 7 h. Next, the cells were fixed in 4% buffered formalin for 5 min, at 37 °C, washed with PBS and permeabilized with 0.1% Triton X-100 in PBS for 10 min at RT. Nonspecific antibody binding was blocked for 10 min (RT) and subsequently incubated with monoclonal anti-α-tubulin antibody produced in mouse (Sigma) diluted 1:2000 for overnight (4 °C). The coverslips were then washed tree times with 0.05% Triton X-100 in PBS and the cells were incubated with secondary antibodies to mouse IgG conjugated with FITC (Sigma) diluted 1:64 for 1 h at RT, washed and counterstained with DAPI (Sigma). Finally, cells were washed with PBS (twice) and mounted on glass slides. The slides were examined with a FV1000 confocal microscope (Olympus, Germany) in two separated channels: for DAPI (405 nm laser), FITC (488 nm laser).

4.2.6. Cell free tubulin polymerization assay

Tubulin polymerization assay was conducted using a fluorescence-based tubulin polymerization kit (BK011P, Cytoskeleton, USA) according to the manufacturer's protocol. The compounds **13a, 13b, 15, 16** (100 μM) and **14** (50 μM) were evaluated for their effect on tubulin polymerization (in cell free conditions). Because of high auto-florescent signal of compound 12b, it was not evaluated in the fluorescence based tubulin polymerization assay. Paclitaxel and vinblastine (3 μM) were used as references and DMSO as a vehicle control. The finally DMSO concentration did not exceed 0.2% in all samples. After incubation of the tested compounds at 37 °C for 1 min, the icy tubulin reaction mixture (2 mg/mL tubulin, 1.0 mM GTP in 80 mM PIPES, 2.0 mM MgCl2, 0.5 mM EGTA and 15% glycerol, pH 6.9) was added. The samples were mixed and tubulin assembly was monitored (excitation: 360 nm, emission: 450 nm) at 1 min intervals for 1 h at 37 °C using a spectrophotometric microplate reader (Infinite 200 Pro, Tecan, Switzerland). The readings were acquired from at least three independent experiments.

Appendix A. Supplementary material

Supplementary data to this article can be found online at https://doi.org/10.1016/j.bioorg.2019.102930.

References

[1] L. Wilson, D. Panda, A. Jordan, Modulation of microtubule dynamics by drugs; A paradigm for the action of cellular regulators, Cell Struct. Function 24 (1999) 329–335.

[2] M.A. Jordan, L. Wilson, Microtubules as a target for anticancer drugs, Nat. Rev. Cancer. 4 (2004) 253–265.

[3] B. Gigant, C. Wang, R.B. Ravelli, F. Roussi, M.O.P. Steinmetz, P.A. Curmi, A. Sobel, M. Knossow, Structural basis for the regulation of tubulin by vinblastine, Nature 435 (2005) 519–522.

[4] J. Qi, H. Dong, J. Huang, S. Zhang, L. Niu, Y. Zhang, J. Wang, Synthesis and biological evaluation of *N*-substituted 3-oxo-1,2,3,4-tetrahydro-quinoxaline-6-carboxylic acid derivatives as tubulin polymerization inhibitors, Eur. J. Med. Chem. 143 (2018) 8–20.

[5] F. Sultana, S.R. Bonam, V.G. Reddy, V.L. Nayak, R. Akunuri, S.R. Routhu, A. Alarifi, M.S.K. Halmuthur, A. Kamal, Synthesis of benzo[*d*]imidazo[2,1-*b*]thiazole-chalcone conjugates as microtubule targeting and apoptosis inducing agents, Bioorg. Chem. 76 (2018) 1–12.

[6] Z.Z. Zhou, X.D. Shi, H.F. Feng, Y.F. Cheng, H.T. Wang, J.P. Xu, J.P. Xu, Discovery of 9*H*-purins as potential tubulin polymerization inhibitors: Synthesis, biological evaluation and structure-activity relationships, Eur. J. Med. Chem. 138 (2017) 1126–1134.

[7] Y. Zhou, W. Yan, D. Cao, M. Shao, D. Li, F. Wang, Z. Yang, Y. Chen, L. He, T. Wang, M. Shen, L. Chen, Design, synthesis and biological evaluation of 4-anilinoquinoline derivatives as novel potent tubulin depolymerization agents, Eur. J. Med. Chem. 138 (2017) 1114–1125.

[8] N.M. O'Boyle, M. Carr, L.M. Greene, O. Bergin, S.M. Nathwani, T. McCabe, D.G. Lloyd, D.M. Zisterer, M.J. Meegan, Synthesis and evaluation of azetidinone analogues of combretastatin A-4 as tubulin targeting agents, J. Med. Chem. 53 (2010) 8569–8584.

[9] C. Dumontet, M.A. Jordan, Microtubule-binding agents: a dynamic field of cancer therapeutics, Nat. Rev. Drug Discov. 9 (2010) 790–803.

[10] K.N. Bhalla, Microtubule-targeted anticancer agents and apoptosis, Oncogene 22 (2003) 9075–9086.

[11] J. Chen, T. Liu, X. Dong, Y. Hu, Recent developments and SAR analysis of colchicine binding site inhibitors, Mini-Rev. Med. Chem. 9 (2009) 1174–1190.

[12] Y. Lu, J. Chen, M. Xiao, W. Li, D.D. Miller, An overview of tubulin inhobitors that interact with the colchicine binding site, Pharm. Res. 29 (2012) 2943–2971.

[13] G. Nagaiah, S.C. Remick, Combretastatin A4 phosphate: a novel vascular disrupting agent, Future Oncol. 6 (2010) 1219–1228.

[14] G.J. Rustin, G. Shreeves, P.D. Nathan, A. Gaya, T.S. Ganesan, D. Wang, J. Boxall, L. Poupard, D.J. Chaplin, M.R.L. Stratford, J. Balkissoon, M. Zweifel, A phase Ib trial of CA4P (combretastatin A-4 phosphate), carboplatin, and paclitaxel in patients with advanced cancer, Br. J. Cancer. 102 (2010) 1355–1360.

[15] D.M. Patterson, G.J.S. Rustin, N. Serradell, E. Rosa, J. Bolos, Combretastatin A-4 phosphate, Drugs Future 32 (2007) 1025–1032.

[16] B.L. Flynn, G.S. Gill, D.W. Grobelny, J.H. Chaplin, D. Paul, A.F. Leske, T.C. Lavranos, D.K. Chalmers, S.A. Charman, E. Kostewicz, D.M. Shackleford, J. Morizzi, E. Hamel, M.K. Jung, G. Kremmidiotis, Discovery of 7-hydroxy-6-methoxy-2-methyl-3-(3,4,5-trimethoxybenzoyl)benzo[b]furan (BNC105), a tubulin polymerization inhibitor with potent antiproliferative and tumor vascular disrupting properties, J. Med. Chem. 54 (2011) 6014–6027.

[17] D. Rischin, D.C. Bibby, G. Chong, G. Kremmidiotis, A.F. Leske, C.A. Matthews, S.S. Wong, M.A. Rosen, J. Desai, Clinical, pharmacodynamic, and pharmacokinetic evaluation of BNC105P: a phase I trial of a novel vascular disrupting agent and inhibitor of cancer cell proliferation, Clin. Cancer Res. 17 (2011) 5152–5160.

[18] H. Khanam, Shamsuzzaman, Bioactive Benzofuran derivatives: A review, Eur. J. Med. Chem 97 (2015) 483–504.

[19] H. Kwiecień, M. Śmist, M. Kowalewska, Recent development on the synthesis of benzo[*b*]- and naphtho[*b*]furans: a review, Curr. Org. Synth. 9 (2012) 529–560.

[20] R. Naik, D.S. Harmalkar, X. Xu, K. Jang, K. Lee, Bioactive benzofuran derivatives: moracins A-Z in medical chemistry, Eur. J. Med. Chem. 90 (2015) 379–393.

[21] S.F. Wu, F.R. Chang, S.Y. Wang, T.L. Hwang, C.L. Lee, S.L. Chen, C.C. Wu, Y.C. Wu, Anti-inflamatory an cytotoxic neoflavonoids and benzofurans from Pterocarpus santalinus, J. Nat. Prod. 74 (2011) 989–996.

[22] H.F. Fan, Y.M. Ren, X.L. Wu, Q.A. Wang, Synthesis and cytotoxicity of novel benzofuran neoligands derivatives, J. Chem. Res. 34 (2010) 233–235.

[23] S. Parekh, D. Bhavsar, M. Savant, S. Thakrar, A. Bavishi, M. Parmar, H. Vala, A. Radadiya, N. Pandya, J. Serly, J. Molnár, A. Shah, Synthesis of some novel benzofuran-2-yl(4,5-dihydro-3,5-substituted diphenylpyrazol-1-yl) methanones and studies on the antiproliferative effects and reversal of multidrug resistance of human MDR1-gene transfected mouse lymphoma cells in vitro, Eur. J. Med. Chem. 46 (2011) 1942–1948.

[24] M.A. Bazin, L. Bodero, C. Tomasoni, B. Rousseau, C. Roussakis, P. Marchand, Synthesis and antiproliferative activity of benzofuran-based analoges of cercosporamide against non-small cell lung cancer lines, Eur. J. Med. Chem. 69 (2013) 823–832.

[25] S.T. Hazeldine, L. Polin, J. Kushner, K. White, T.H. Corbett, J.P. Horwitz, Synthesis and biological evaluation of conformationally constrained analogs of the antitumor agents XK469 and SH80. Part 5, Bioorg. Med. Chem. 14 (2006) 2462–2467.

[26] I. Hayakawa, R. Shioya, T. Agatsuma, H. Furukawa, Y. Sugano, Thienopyridine and benzofuran derivatives as potent anti-tumor agents possessing different structure-activity relationships, Bioorg. Med. Chem. Lett. 14 (2004) 3411–3414.

[27] I. Hayakawa, R. Shioya, T. Agatsuma, H. Furukawa, S. Narutoc, Y. Sugano, A library synthesis of 4-hydroxy-3-methyl-6-phenylbenzofuran-2-carboxylic acid ethyl ester derivatives as anti-tumor agents, Bioorg. Med. Chem. Lett. 14 (2004) 4383–4387.

[28] K. Bao, A. Fan, Y. Dai, L. Zhang, W. Zhang, M. Cheng, X. Yao, Selective demethylation and debenzylation of aryl ethers by magnesium iodide under solvent-free conditions and its application to the total synthesis of natural products, Org. Biomol. Chem. 7 (2009) 5084–5090.

[29] A.S. Negi, S.K. Chattopadhyay, S. Srivastava, A.K. Bhattacharya, A simple regioselective demethylation of *p*-Aryl methyl ethers using aluminum chloride-dichloromethane system, Synth. Commun. 35 (2005) 15–21.

[30] H. Kwiecień, M. Szychowska, Synthesis and reduction of 5-halo- and 5- nitro-1-(benzofuran-3-yl)-2-phenylethanones, Chem. Heterocyclic Comp. 8 (2006) 1158–1166.

[31] H. Kwiecień, E. Baumann, Benzofuran systems. Synthesis and biological examination of 1-(3-Benzofuranyl)-2-phenylethanones, J. Heterocyclic Chem. 34 (1997) 1587–1590.

[32] H. Kwiecień, E. Baumann, Benzofuran systems. Regioselective bromintion and some other reactions of 1-(3-benzofuranyl)-2-phenylethanones, J. Heterocyclic Chem. 35 (1998) 1501–1503.

[33] R. Romagnoli, P.G. Baraldi, T. Sarkar, C.L. Cara, O.C. Lopez, M.D. Carrion, D. Preti, M. Tolomeo, J. Balzarini, E. Hamel, Synthesis and biological evaluation of 2-aroyl-4-phenyl-5-hydroxybenzofurans as a new class of antitubulin agents, Med Chem. 4 (2008) 558–564.

[34] R. Romagnoli, P.G. Baraldi, T. Sarkar, M.D. Carrion, O. Cruz-Lopez, C. Lopez Cara, M. Tolomeo, S. Grimaudo, A. Di Cristina, M.R. Pipitone, J. Balzarini, R. Gambari, L. Ilaria, R. Saletti, A. Brancale, E. Hamel, Synthesis and biological evaluation of 2-(3′,4′,5′ trimethoxybenzoyl)-3-N, N-dimethylamino benzo[b]furan derivatives as

inhibitors of tubulin polymerization, Bioorg. Med. Chem. 16 (2008) 8419–8426.
[35] R. Romagnoli, P.G. Baraldi, M.D. Carrion, C.L. Cara, O. Cruz-Lopez, M. Tolomeo, S. Grimaudo, A. Di Cristina, M.R. Pipitone, J. Balzarini, N. Zonta, A. Brancale, E. Hamel, Design, synthesis and structure-activity relationship of 2-(3',4',5'-trimethoxybenzoyl)-benzo[b]furan derivatives as a novel class of inhibitors of tubulin polymerization, Bioorg. Med. Chem. 17 (2009) 6862–6871.
[36] A. Kamal, N.V. Reddy, V.L. Nayak, V.S. Reddy, B. Prasad, V.D. Nimbarte, V. Srinivasulu, M.V. Vishnuvardhan, C.S. Reddy, Synthesis and biological evaluation of benzo[b]furans as inhibitors of tubulin polymerization and inducers of apoptosis, Chem. Med. Chem. 9 (2014) 117–128.
[37] W.T. Brady, Y.S.F. Giang, A.P. Marchand, A.H. Wu, Intramolecular [2 + 2] cycloadditions of ketenes to carbonyl groups. A novel synthesis of substituted benzofurans, J. Org. Chem. 52 (1987) 3457–3461.
[38] E. Klein, S. DeBonis, B. Thiede, D.A. Skoufias, F. Kozielski, L. Lebeau, New chemical tools for investigating human mitotic kinesin Eg5, Bioorg. Med. Chem. 15 (2007) 6474–6488.